ADVANCED MODELLING-BASED METHODOLOGY FOR EVALUATION AND DESIGN OF LARGE REFLECTOR ANTENNAS FOR SPACE APPLICATIONS - STATE-OF-THE-ART AND COLLABORATIVE RESEARCH PERSPECTIVE

Wojciech Gwarek, Malgorzata Celuch, Marzena Olszewska – Placha

QWED Sp z o.o., ul. Krzywickiego 12 lok.1, 02-078 Warszawa, Poland, Email: wgwarek@qwed.eu

Abstract **–** This work aims to popularise a modelling-based methodology for the design of antenna systems. Our in-house conformal FDTD algorithms in full 3D and BOR V2D formulations are amalgamated in the commercial QW-3D and QW-V2D packages, respectively. QW-V2D provides unique functionalities for the full-wave modelling of large axisymmetrical dual-reflector as well as dual-mode antennas, scaling to over 3000 wavelength. Applications of QW-3D to waveguide components of antenna feeds are illustrated with ALMA project memos and further extend to polarisers, diplexers, and OMTs. At the workshop we shall demonstrate co- and post-processing techniques, which produce key engineering parameters but also allow direct insight into EM near-field distributions and thereby reveal otherwise invisible causes of, e.g., spillover. We also discuss applications of QW-V2D in material measurement techniques, with focus on our own dielectric resonator setups.

I. THE FDTD BOR METHOD

It has been proven [1] that the structures maintaining axial symmetry of boundary conditions (so-called Bodies of Revolution, BOR) belong to the class of vector two - dimensional (V2D) problems. The total electromagnetic field in such structures can be decomposed into a series of orthogonal modes, of different angular field dependence of the $\cos(n\varphi)$ or $\sin(n\varphi)$ type, where φ is the angular variable of the cylindrical coordinate system and n=0,1,2… Thereby the numerical analysis can be conducted in two space dimensions, over one half of the long-section of the structure, with n predefined as a parameter. The BOR formulation of our in-house conformal FDTD method has been implemented as the QW-V2D package of QuickWave software family [2].

Note that the n-mode defined above should not be confused with one mode of a circular waveguide. For example, one QW-V2D analysis with n=1 takes into account a composition of all circular waveguide modes TE1k and TM1m, where k and m are arbitrary natural numbers.

The equations describing E- and H- fields in a BOR structure are identical to the equations in a planar circuit with appropriate transformation of fields and media parameters, as shown in Fig. 1. Not repeating the formalism of those transformations available in [1][3], let us point out that:

- The equivalent structure of Fig. 1b is filled with an anisotropic and inhomogeneous (y'-dependent) medium.
- Tangential (x', y') field components of Fig. 1b correspond directly to the longitudinal and radial components of Fig. 1a, while the vertical (z') components correspond to the angular component of Fig. 1a multiplied by its radial position.
- The angular variation n is related in Fig. 1b the mode number in the z' direction.

In a general case the structure as in Fig. 1b cannot support pure TM and TE modes. The fields can be described by a vector 2D wave equation, which justifies the name QW-V2D for the presented software. BOR structures are scalar 2D problems for n=0 and V2D structures for n>0. There also exist non-BOR structures, which can be assigned to the V2D class and can be analysed with the QuickWave software, but this work elaborates on BOR V2D problems only.

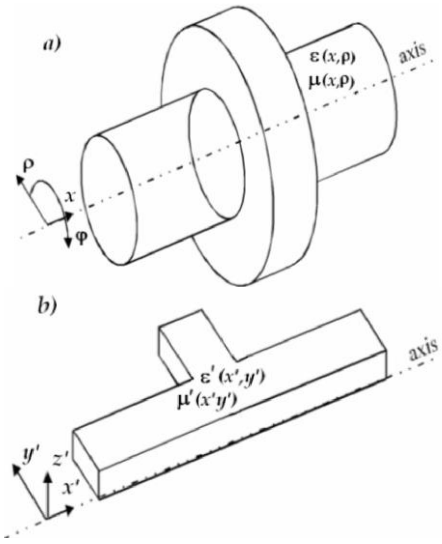

Figure 1: Equivalence between planar and BOR

circuits. A planar equivalent of the BOR circuit is filled with inhomogeneous anisotropic materials.

Since the equivalent planar circuit of Fig. 1b is an inhomogeneous structure with diagonal anisotropy of materials, it is a natural candidate for the FDTD method. However, classical FDTD algorithms suffer from limited geometrical accuracy due to their stair-case approximation of material boundaries, which are crucial in the modelling of horn antennas and their reflectors. That disadvantage has been resolved in QW-V2D as shown in Fig. 2, which presents a fragment of the internally generated FDTD mesh. There we can see three materials: metal, air, and a dielectric. Three basic meshing mechanisms have been applied:

- Variable non-equidistant mesh is snapped to the edges.
- Any boundary cell is conformally divided between two media by a straight line tangential to the physical boundary passing arbitrarily through the cell. Unique to QuickWave is an algorithm that merges small parts of a cell remaining from that kind of division directionally to its adjacent cells. Thereby the conformal mesh does not require FDTD time step reduction and retains the basic algorithm efficiency. In terms of accuracy it outperforms other reported FDTD schemes [4].
- Though not visible in Fig. 2, QW-V2D further imposes field singularity corrections to EM field components adjacent to the metal edges and corners [5].

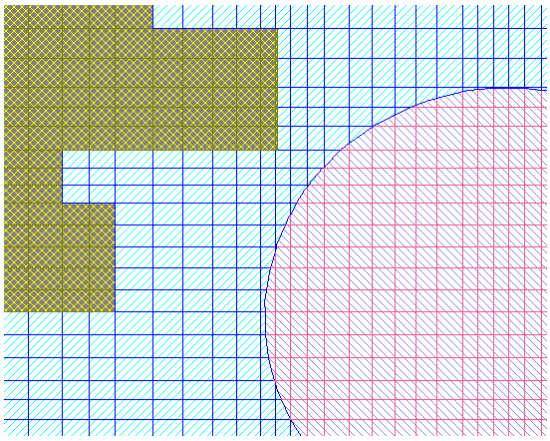

Figure 2: Example of conformal meshing applied in QW-V2D. Each cell can be divided between two media by an arbitrarily passing straight line. Variable mesh is fitted to edges and corners. Singularity models are imposed in cells surrounding metal edges and corners.

II. A Compact Dual Reflector Antenna

In this section we consider QW-V2D application to the analysis of a compact dual reflector antenna as in Fig. 3. The antenna is designed for 8.2 GHz and the diameter of the main reflector is 610 mm. Thus the reflector size is about 16.4 λ. On the left we can see a general view of the antenna, while on the right we can see it in the QW-V2D Editor [2], where half of its long section is presented. Around the antenna there is an absorbing boundary (in blue) and a pick-up surface for near-to-far (NTF) field transformation after [6]. Metal parts of the antenna are pictured in dark green, while the dielectric part supporting the sub-reflector is shown in red. The sub-reflector is quite small. Its diameter equals to about 2.8 λ. That is why its shape as shown in Fig. 3b (and zoomed in Fig. 4) is quite different from the one expected from quasi - optical approximation. Nevertheless it well serves the assumed design target, as seen from Fig. 5 which displays the E-plane and H-plane radiation patterns at 7.8 GHz and 8.2 GHz. The gain is 32.2 dB and 32.6 dB, respectively. There are relatively small side lobes and above 20 degrees the radiation is more than 38 dB below the main beam. The matching of the antenna is analysed in Fig. 6.

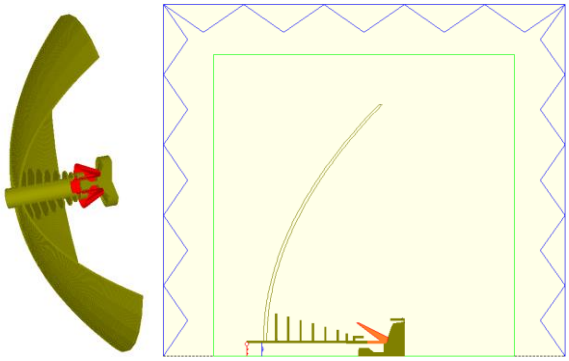

Figure 3: The compact dual horn antenna modelled in QW-V2D: overall view (left) and its half - section considered in QW-V2D with the absorbing boundary and the NTF pick-up surface.

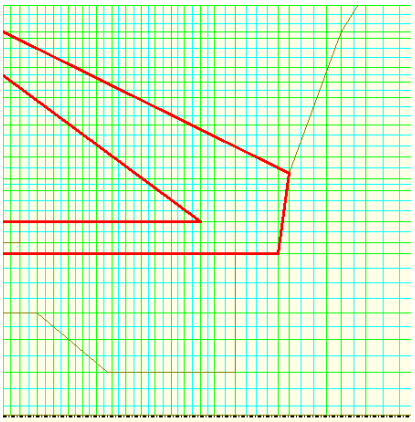

Figure 4: Fragment of antenna meshing in QW-V2D: the dielectric support is marked with a thick red line.

Let us now discuss the computer effort required for the discussed simulation. Following the guidelines due to numerical dispersion bounds [7] and the meshing mechanisms listed in Section I, we have applied the basic FDTD cell size of 1/20 λ, and variable mesh refined to about 1/50 λ in sensitive parts of the antenna. A fragment of the mesh close to the dielectric support is

shown in Fig. 4. The full model comprises 116 000 FDTD cells. Since approximately 100 Bytes are needed for one FDTD cell, the estimated total memory needed for the simulation data is about 11 MB. On top of that, we need to take into account the processing code (about 40 MB) and the storage of graphics (typically 5 to 40 MB depending on the number and type of the opened windows, of which field displays are most consuming).

There are several options of the QW-V2D engine including three basic ones: sequential (performing sequential CPU operations), OMP (using the system multiprocessor / multicore processing abilities), and GPU (processing on graphic cards). More information about those processing options will be given in Section III. Here, we have started the simulation using an average laptop computer equipped with Intel Core I5 processor and NVIDIA GeForce GT 540M graphic card. We have observed the following speeds of simulation of the considered example, expressed in the number of FDTD iterations per second:

- sequential version - 350
- OMP version – 600
- GPU version – 640.

The full-frequency-band results of Fig. 5 and Fig. 6 have been obtained after about 10 000 iterations. Thus the total simulation time ranged from 28 seconds with the sequential version down to 16 seconds with the GPU version.

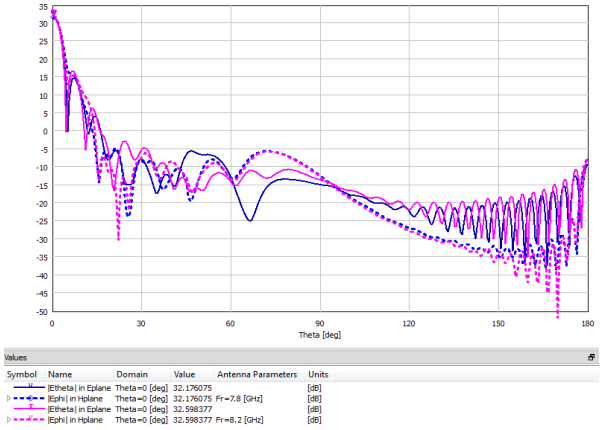

Figure 5: Simulated radiation patterns of the antenna of Fig. 3: in E-plane (continuous) and H-plane (dotted) for the frequencies 7.8 (blue) and 8.2 (magenta) GHz.

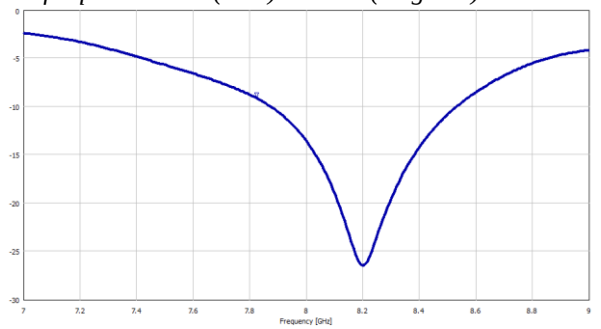

Figure 6: Simulated return loss of the antenna of Fig. 3 (|S11| versus frequency in 7÷9 GHz band).

III. How Big Scenarios Can Be Modelled

The example described in Section II is relatively small, with reflector diameter of the size of 16.4 λ leading to the model of 116 000 FDTD cells. Here we will consider the QW-V2D performance for larger circuits. What happens when we have a larger circuit with reflector size of 80λ or 240λ - is such a problem still solvable on an average computer? We will need to retain the basic meshing of 20 cells per wavelength. Thus the required computer resources will be the same as in the case of the previously considered example over-meshed by a factor of 5 (case a) below) and 15 (case b) below), respectively.

Here are the results of the "over-meshed" experiments:

a) Basic meshing 100 cells/λ; 2.2 Mcells requiring 242 MB of RAM; speed depending on version (in iter/s): sequential-17, OMP-34, GPU-55.

b) Basic meshing 300 cells/λ; 19 Mcells requiring 1.7 GB of RAM; speed depending on version (in iter/s): sequential-2, OMP-4, GPU-6.5.

We conclude that QW-V2D running on our average laptop will allow us to analyse BOR structures with reflector diameters of the order of 240 λ. A larger structure requires a proportionally larger number of FDTD iterations for producing final results. Thus our 240 λ problem would require about 150 000 iterations resulting in the computer time of approximately 380 min, which sounds reasonable for an overnight task.

It is advisable that bigger examples are simulated on mainframe computers, where better speed of processing and bigger memory are available. There is one commonly accepted "figure of merit" for comparing different hardware in application to FDTD codes. It is the number *N* equal to:

$$N = \frac{(number\ of\ FDTD\ cells) * (number\ of\ iterations\ run)}{simulation\ time\ [\mathrm{sec}]} \quad (1)$$

Number *N* depends to some extend on the circuit characteristics (for example, if it is lossy) and the number and type of co- and post-posstprocessing algorithms. Here for reference, we shall assume a lossless circuit with calculations of S11 versus frequency at 100÷1000 frequency points and NTF transform for calculation of radiation patterns at two frequencies as in Section II. For our previously used laptop the number *N* is equal to

- about $40*10^6$ for the sequential version (with little influence of the actual number of FDTD cells in the model),
- varying between $75*10^6$ and $123*10^6$ (depending on the number of cells in the model) for the GPU version.

We shall now run the same example on a mainframe

computer equipped with the CPU Intel i7 4930-K @3.4GHz and 64 GB of RAM, and with GPU card NVIDIA GeForce GTX Titan with memory of 6GB. We start from the meshing of 300 cells / λ considered in point b) above. We observe the speed of 10 iter/s making N=190*10^6 on CPU OMP version and 91 iter/s making N=1729*10^6 on GPU version. Hence the GPU version is expected to provide the return loss and radiation pattern characteristics of an antenna system with the reflector diameter of 240 λ in just about 27 minutes.

We have also checked that with the GPU limit of 6 GB we can run scenarios with the reflector diameter of about 530 λ, taking about 250 minutes of computing time and leading to N=1840*10^6 (slightly higher than in the previous run). When we need to run even bigger scenarios, we should try one of the new multi CPU computers and/or computers equipped with multiple GPU cards. Those computers can be expected to handle the sizes of about 3000 λ while the sizes of 5000 λ seem to be within the high-level state-of-the-art. Fig. 7 shows the performance (described by the value of N) of some common CPU and GPU configurations after [8].

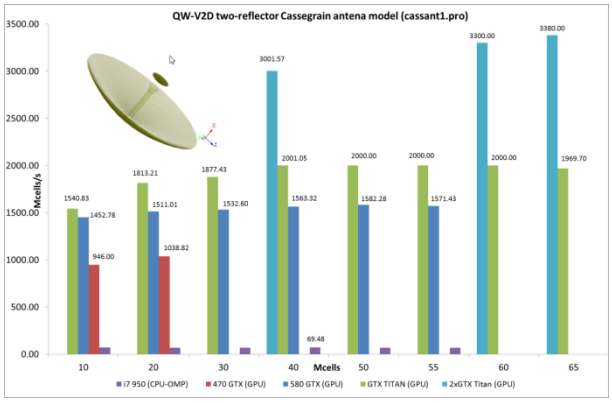

Figure 7: Comparison of performance of QW-V2D software expressed in the value of the "figure of merit N" for different popular CPU and GPU hardware.

We are often asked by prospect software users about the kind of hardware best suitable for FDTD simulations. Our investigations show the dominant hardware parameter influencing the speed of FDTD simulation is *memory bandwidth*, describing the how fast we can transfer a number to and from the memory. The speed of performing the floating point operations influences the speed of the algorithm typically no more than by 5%. As an example: our NVIDIA GeForce GTX Titan graphic card has memory bandwidth of 288 GB/s and produced in our simulation the figure of merit N close to 1.84 10^9. In other words, we needed about 156 B/s for a unit of N. That "rule of thumb" can be used for *a priori* estimation of QW-V2D performance on a computer we plan to use.

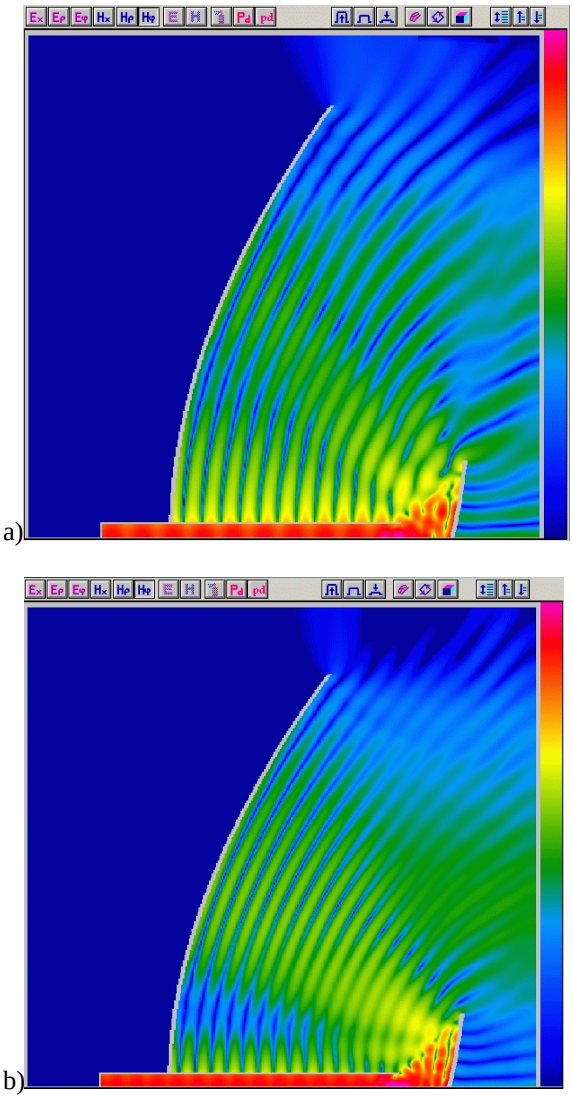

Figure 8: Maximum value of H_φ field in steady state operation of a dual-reflector antenna in logarithmic scale from maximum (purple) down to -60 dB (blue), at 11.7 GHz (a) and 14.1 GHz (b).

IV. Further Advantages of QW-V2D Modelling of Antennas

A. *Visualisation of field patterns*

The applied method of analysis provides direct access to all kinds of field distribution inside the analysed antenna structure, including for example maximum E-field values needed to investigate power limits of transmitting antennas. Field distributions can also be valuable in the analysis of physical causes of undesirable performance. One example is shown in Fig. 8. In that antenna it has been noticed that the side radiation (so called spillover) strongly depends on frequency. It is much bigger at 11.7 GHz than at

14.1 GHz. The field distributions in Fig. 8 provide an important hint as to the cause of such a behaviour. At 11.7 GHz an open - air resonator (a kind of a Fabry - Perrot) is formed along the input guide. It produces strong diffraction at the edge of the sub-reflector leading to radiation perpendicular do the desired direction. Inspired by that observation, we have subsequently corrected the antenna performance by introducing corrugations along the input guide.

B. Direct modelling of dielectric and metal losses

The FDTD simulation method is easily applicable to lossy structures. We can take into account not only lossy dielectrics [7] but also lossy metals [9]. QW-V2D incorporates a wide-band model of the skin effect in metals. Thus we can model both the feeding guide and the reflector built of metals of a particular conductivity. We may investigate the influence of that conductivity on its input and radiation characteristics as well as distribution of the dissipated power inside antenna.

C. Modelling of multimode antennas

As mentioned in Section I, in QW-V2D we assume a particular angular variation *n*. With *n*=1 we take into account a composition of all circular waveguide modes TE1*k* and TM1*m*, where *k* and *m* are arbitrary natural numbers. However, QW-V2D can be also run with other values of *n*. In particular, *n*=0 provides access to modes TE0*k* and TM0*m*. The TM0*m* group includes the TEM mode of a coaxial line and thus such a mode can also be considered. Reflector antennas are sometimes used concurrently with two modes. Modes belonging to *n*=0 group (having not only BOR boundary conditions but also BOR fields) form a beam with zero radiation along the reflector axis. Such modes are used for antenna tracking functions. All kinds of multimode antennas including the ones with the tracking functions are in the mainstream of the QW-V2D applications.

V. Modelling Dielectric Resonators with QW-V2D

Dielectric resonators are of high importance in space technology [10]. They have very high Q-factors as well as small size and weight, important for the reduction of the satellite workload. There is a special interest in the modes of high angular number – so called whispering gallery modes [11]. Their analysis is extremely difficult in general-purpose 3D simulation software since the resonant frequencies of modes of different angular variation can be very close. In QW-V2D we chose *a priori* the angular variation number and thus such modes are naturally separated (they do not appear in the same simulation). Due to its computational efficiency, QW-V2D allows calculating resonant frequencies with accuracies better than 10^{-4} in a reasonable computing time [12]. Figs. 9 show examples of simulated E - field patterns for two different modes in a cylindrical resonator having very close resonant frequencies.

a)

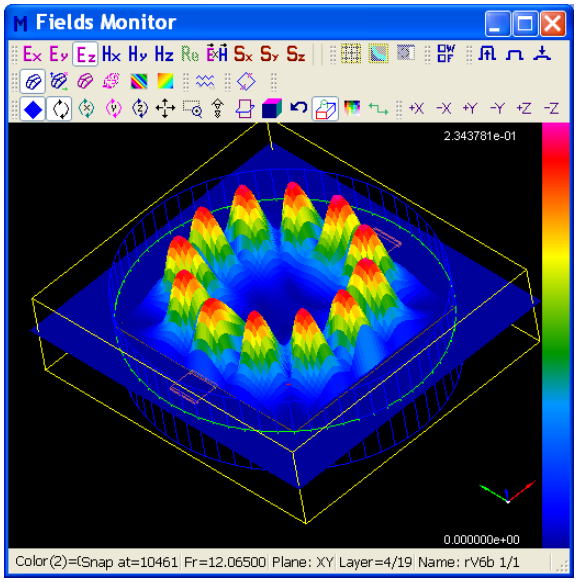

b)

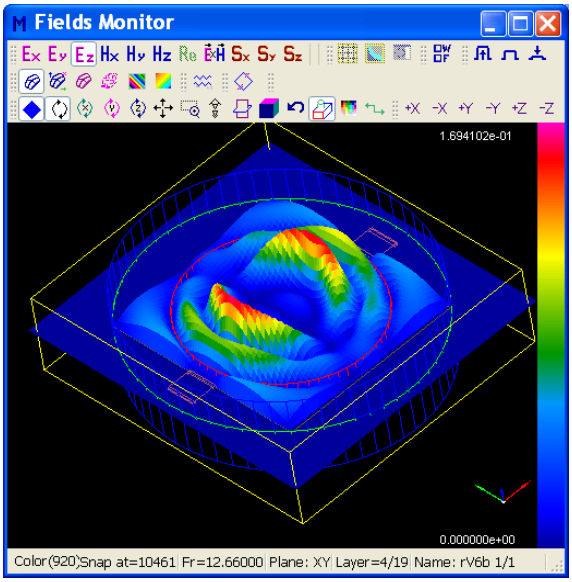

Figure 9: E - field distribution of two modes in a cylindrical dielectric resonator at close resonant frequencies of 12.065 GHz (a) and 12.66 GHz (b).

VI. Applying QW-V2D in Material Measurements

QW-V2D software has also several different applications supporting material measurements at millimeter range. Here are some relevant references:

A. Split-Post Dielectric Resonators (SPDR)

SPDR (Fig. 10) measurements are subject of numerous publications, e.g. [13] leading to popular standards [14].

QW-V2D can be used for preparing look-up tables relating the measured resonant frequencies and Q-factors to the measured material parameters.

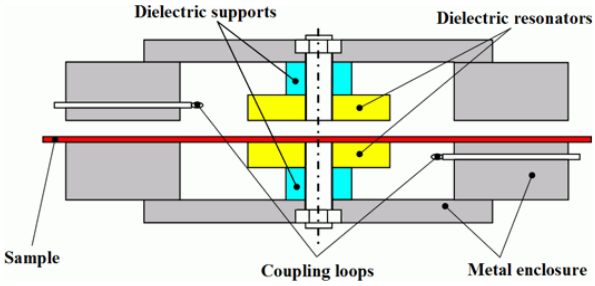

Figure 10: A split - post dielectric resonator (SPDR) [2].

B. Free-space measurements in a Gaussian beam

Fig. 11 shows the QW-V2D model of a horn forming a millimeter-wave Gaussian beam in open air (Fig. 11).

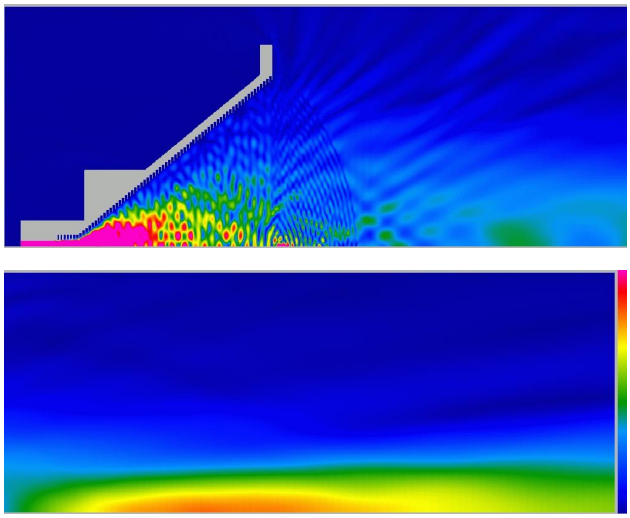

Figure 11: Field distribution close to the corrugated horn with lens, launching the beam (upper picture) and the Gaussian beam waist (formed at some distance) with quasi-TEM wave properties (lower picture).

C. Nanoscale measurements with SMM probes

Scanning Microwave Microscopy (SMM) is an emerging methodology for nanoscale measurements and its accurate modelling has been a subject of interest, also among SMM manufacturers [15]. Extensive research on the SMM, dielectric resonator, free-space, and other microwave material measurement techniques is currently being conducted within the European H2020 MMAMA project [16]. While a complete SMM device is a large and complicated 3D structure, the key microwave interactions with the measured material occur at the tip of the probe, for which a BOR model can be created. In QW-V2D simulations for the model of Fig. 12 we have detected changes of the capacitance at the tip of the probe, depending on the measured material and its depletion layer, at the level of fractions of attofarads. This facilitates better understanding of the microwave phenomena and enhances modelling-based measurements.

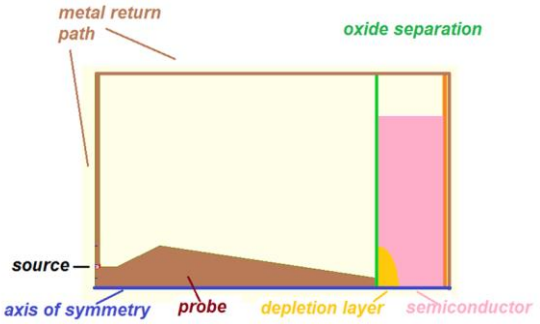

Figure 12: QW-V2D model for the tip of the Keysight SMM probe after [15].

VII. Applying QW-3D to Waveguide Components

While our QW-V2D package presented this far is dedicated to BOR problems, QuickWave family also includes a general-purpose 3D conformal FDTD package called QW-3D [2]. Among its applications are 3D waveguide structures used in microwave and millimeter wave radio-astronomy receivers. Here we are proud to reference several works [17][18][19][20] of the scientists from National Radio Astronomy Observatory of Charlottesville, VA. They describe their designs for the receiver of the Atacama Large Millimeter Array (ALMA) and date to 1999-2001.

Needless to say, the QW-3D package of today can handle larger and more intricate problems, with accuracy and efficiency higher by orders of magnitude, in comparison with those reported in early 2000s. There have been many other designs of antenna feeding systems prepared around the world, wherein QuickWace developers assisted either with interpretations of the simulation results or by developing specific software models and procedures.

VIII. Collaborative Research Perspective

We have outlined the scope of applications of our electromagnetic software of QuickWave series: QW-3D and BOR QW-V2D. The software has been present on the world market for over 20 years. From the very beginning it has been used in radioastronomy and many specific models have been implemented based on the feedback from space researchers. The original authors of QuickWave are still active and seeking new challenges within the European space projects. We offer insider expertise in the use of QuickWave modelling

tools. We are also open to introduce new task - oriented modifications of QuickWave software.

IX. Acknowledgement

The work leading to this paper has received funding from the European Union Horizon H2020 Programme (H2020-NMBP-07-2017) under grant agreement n°761036.

X. References

[1] Gwarek, W.K., Morawski, T. & Mroczkowski, C. (1992). Application of the FD-TD Method to the Analysis of Circuits Described by the Two-Dimensional Vector Wave Equation. *IEEE Trans.Microwave Theory Tech.*, **41**(2), pp311-317.

[2] QuickWave EM Software (1997-2018). On-line at: www.qwed.eu (as of 28 August 2018).

[3] Celuch, M. & Gwarek, W.K. (2008). Industrial design of axisymmetrical devices using a customized FDTD solver from RF to optical frequency bands. *IEEE Microwave Mag.*, **9**(6), pp150-159.

[4] Celuch - Marcysiak, M. (2001). Evaluation and Enhancement of Supraconvergence Effects on Nonuniform and Conformal FDTD meshes. In *IEEE MTT-S Intl. Microwave Symp. Dig.*, Phoenix, AZ, US, pp745-748.

[5] Celuch - Marcysiak, M. (2003). Local Stereoscopic Field Singularity Models for FDTD Analysis of Guided Wave Problems. In *IEEE MTT-S Intl. Microwave Symp. Dig.*, Philadelphia, PA, pp1137-1140.

[6] Mroczkowski, C., Celuch - Marcysiak, M. & Gwarek, W.K. (1994). Joint Application of Superabsorption and Near-to-Far Field Transform to FDTD Analysis of Axisymmetrical Antennas. In *Proc. 24th Eur. Microwave Conf.*, Cannes, FR, pp899-904.

[7] Celuch - Marcysiak, M. (2004). Extended Theory of FDTD S- and P-Eigenmodes in Lossy Media and Its Application to the Analysis of Coupled Problems. In *IEEE MTT-S Intl. Microwave Symp. Dig.*, Fort Worth, AZ, pp1713-1716.

[8] Sypniewski, M & Celuch, M. (2015). Optimization of the Electromagnetic FDTD Simulation Performance (in Polish). *Elektronika : konstrukcje, technologie, zastosowania*, **56**(7), Wyd. SIGMA-NOT, pp30-34.

[9] Celuch - Marcysiak, M., Gwarek, W. & Sypniewski, M. (1998). A Simple and Effective Approach to FD-TD Modelling of Structures Including Lossy Metals. In *IEEE Asia-Pacific Microwave Conf. Proc.*, Yokohama, JP, pp991-993.

[10] Fiedziuszko, S.J (1982). Dual-Mode Dielectric Resonator Loaded Cavity Filters. *IEEE Trans. Microwave Theory Tech.*, **30**(9), pp1311-1316.

[11] Krupka, J., Derzakowski, K., Abramowicz, A., Tobar, M.E. & Geyer, R. (1999). Use of Whispering-Gallery Modes for Complex Permittivity Determinations of Ultra-Low-Loss Dielectric Materials. *IEEE Trans. Microwave Theory Tech.*, **47**(6), pp752-759.

[12] Gwarek, W. & Celuch, M. (2018). Accurate Analysis of Whispering Gallery Modes in Dielectric Resonators with BoR FDTD Method. In *Proc. 22nd Intl. Microwave & Radar Conf. MIKON*, Poznan, PL, pp302-303.

[13] Krupka, J., Gragory, A.P., Rochard, O.C., Clarke, R.N.,Riddle, B. & Baker - Jarvis, J. (2001). Uncertainty of Complex Permittivity Measurements by Split-Post Dielectric Resonator Technique. *J. Eur. Ceramic Soc.*, **21**(15), pp2673-2676.

[14] International Standard IEC 61189-2-721 (2015). IEC, Geneva, CH.

[15] Oladipo, A.O., Kasper, M., Lavdas, S., Gramse, G., Kienberger, F. & Panoiu, N.C. (2013). Three-Dimensional Finite-Element Simulations of a Scanning Microwave Microscope Cantilever for Imaging at the Nanoscale. *Appl. Phys. Lett.*, **103**(213106).

[16] MMAMA, Microwave Microscopy for Advanced and Efficient Materials Analysis and Production. The European Union Horizon H2020 Programme project. Online at (as of 28 August 2018): www.mmama.eu

[17] Kerr, A.R, Wollack, E. & Horner, N. (1999). Waveguide Flanges for ALMA Instrumentation. *ALMA Memo No.278*. Online at (as of 29 August 2018): http://library.nrao.edu/public/memos/alma/main/memo278.pdf

[18] Kerr, A.R. & Horner, N. (2000). A Broadband In-Phase Waveguide Power Divider/Combiner. *ALMA Memo No.325*. Online at (as of 29 August 2018): http://library.nrao.edu/public/memos/alma/main/memo325.pdf

[19] Srikanth, S. & Kerr, A.R. (2001). Waveguide Quadrature Hybrids for ALMA Receivers. *ALMA Memo No.343*. Online at (as of 29 August 2018): http://library.nrao.edu/public/memos/alma/main/memo343.pdf

[20] Kerr, A.R. (2001). Elements for E-Plane Split-Block Waveguide Circuits. *ALMA Memo No.381*. Online at (as of 29 August 2018): http://library.nrao.edu/public/memos/alma/main/memo381.pdf